Orphan nuclear receptor NGFI-B forms dimers with nonclassical interface

MARCOS R. CALGARO,[1,5] MARIO DE OLIVEIRA NETO,[1,5] ANA CAROLINA M. FIGUEIRA,[1,5] MARIA A.M. SANTOS,[1] RODRIGO V. PORTUGAL,[1] CAROLINA A. GUZZI,[1] DANIEL M. SAIDEMBERG,[2] LUCAS BLEICHER,[1] JAVIER VERNAL,[3] PABLO FERNANDEZ,[4] HERNÁN TERENZI,[3] MARIO SERGIO PALMA,[2] AND IGOR POLIKARPOV[1]

[1]Instituto de Física de São Carlos, Departamento de Física e Informática, Universidade de São Paulo, CEP 13566-590 São Carlos, São Paulo, Brazil
[2]Laboratório de Biologia Estrutural e Zooquímica, CEIS, Universidade Estadual de São Paulo, CEP 13500-230 Rio Claro, Brazil
[3]Laboratório de Expressão Gênica, Departamento de Bioquímica, Universidade Federal de Santa Catarina, 88040-900 Florianópolis, São Carlos, Brazil
[4]Unité d'Expression des Genes Eucaryotes, Institut Pasteur, 75015 Paris, France

(RECEIVED November 28, 2006; FINAL REVISION April 21, 2007; ACCEPTED May 1, 2007)

Abstract

The orphan receptor nerve growth factor-induced B (NGFI-B) is a member of the nuclear receptor's subfamily 4A (Nr4a). NGFI-B was shown to be capable of binding both as a monomer to an extended half-site containing a single AAAGGTCA motif and also as a homodimer to a widely separated everted repeat, as opposed to a large number of nuclear receptors that recognize and bind specific DNA sequences predominantly as homo- and/or heterodimers. To unveil the structural organization of NGFI-B in solution, we determined the quaternary structure of the NGFI-B LBD by a combination of ab initio procedures from small-angle X-ray scattering (SAXS) data and hydrogen–deuterium exchange followed by mass spectrometry. Here we report that the protein forms dimers in solution with a radius of gyration of 2.9 nm and maximum dimension of 9.0 nm. We also show that the NGFI-B LBD dimer is V-shaped, with the opening angle significantly larger than that of classical dimer's exemplified by estrogen receptor (ER) or retinoid X receptor (RXR). Surprisingly, NGFI-B dimers formation does not occur via the classical nuclear receptor dimerization interface exemplified by ER and RXR, but instead, involves an extended surface area composed of the loop between helices 3 and 4 and C-terminal fraction of the helix 3. Remarkably, the NGFI-B dimer interface is similar to the dimerization interface earlier revealed for glucocorticoid nuclear receptor (GR), which might be relevant to the recognition of cognate DNA response elements by NGFI-B and to antagonism of NGFI-B–dependent transcription exercised by GR in cells.

Keywords: orphan nuclear receptor; NGFI-B; glucocorticoid nuclear receptor; hydrogen–deuterium exchange; SAXS

The nuclear receptor (NR) superfamily is composed of ligand-dependent transcription factors which play important roles in cell growth, differentiation, metabolism, reproduction, and morphogenesis of higher organisms, including humans. The nuclear receptors reside in either the cytoplasm or nucleus, and activate transcription in

[5]These authors contributed equally to this work.

Reprint requests to: Igor Polikarpov, Instituto de Física de São Carlos, Departamento de Física e Informática, Universidade de São Paulo, Avenida Trabalhador São Carlense, 400, CEP 13566-590 São Carlos, SP, Brazil; e-mail: ipolikarpov@if.sc.usp.br; fax: +55-16-3373-9881.

Article published online ahead of print. Article and publication date are at http://www.proteinscience.org/cgi/doi/10.1110/ps.062692207.

response to specific lipophylic ligands such as steroids, thyroid hormones, retinoids, vitamin D, prostaglandins, fatty acids, and other ligands (Ribeiro et al. 1995, 1998). Practically all nuclear receptors have a modular structure which consists of three major domains: the N-terminal domain, the most variable in size and sequence (Shao and Lazar 1999); the DNA-binding domain (DBD), the most conserved part of the protein, which confers the ability to recognize specific DNA sequences (Lee et al. 1993); and the C-terminal part, a multifunctional domain responsible for ligand-dependent transcriptional activation (LBD) (Wurtz et al. 1996). So far, 48 different nuclear receptors have been identified in the human body, and for a number of them, the biochemical bases for activity and their cognate ligands have been elucidated. However, for some orphan nuclear receptors, including NGFI-B, physiologically relevant ligands have not been identified to date (Giguere 1999).

The NGFI-B or Nr4a1 in standard classification (also called TR3, Nur77, NAK1, and eight other aliases) belongs to the nuclear receptor subfamily 4A (Nr4a) which also includes two other receptors: Nurr1/Nr4a2 and NOR-1/Nr4a3 (Herschman 1991; Maruyama et al. 1998). Members of this subgroup exhibit significant similarity in their DNA-binding domains, moderate similarity in their ligand (like)-binding and transactivation domains (Giguere 1999), and all play important roles in the nervous, endocrine, and immune systems. All three receptors are immediate–early response gene products that are induced after stimulation with serum, growth factors, and nerve growth factor (NGF) (Hazel et al. 1988; Milbrandt 1988). Similarly to many other orphan nuclear receptors, the members of the subfamily 4A regulate the expression of other genes, ultimately culminating in phenotypic changes (Herschman 1991). They do so by binding, either as monomers to a consensus NBRE sequence (AAAGGTCA) upstream to the target gene (Wilson et al. 1991), or as homodimers activating transcription through the Nur-responsive elements (NurRE, widely spaced everted repeat of AAAT[G/A][C/T]CA separated by 10 base pairs) (Philips et al. 1997a). The expression of NGFI-B, NOR-1, or Nurr1 alone is sufficient to activate NBRE or NurRE-directed transcriptional activities. In addition, recent studies have shown that they also heterodimerize with each other (Maira et al. 1999) and that NGFI-B and Nurr1, but not NOR-1, can also activate transcription through DR5 elements (AGGTCA n AGGTCA; $n = 5$), acting as heterodimers with the retinoid X receptor (RXR) (Forman et al. 1995; Perlmann and Jansson 1995). Therefore, NGFI-B and related transcription factors function through a variety of genetic targets participating in multiple roles in both developmental and physiological regulation.

NGFI-B is widely expressed and was originally identified by virtue of its rapid induction by serum in fibroblasts and by NGF in cell line PC12 (Hazel et al. 1988). NGFI-B is involved in distinct cellular functions, such as differentiation of neural cells (Saucedo-Cardenas et al. 1998), modulation of retinoic acid signal transduction (Perlmann and Jansson 1995), and regulation of steroidogenesis in the human adrenal cortex (Lu et al. 2004). The importance of NGFI-B in the apoptotic process was earlier demonstrated in knockout experiments in T-cell hybridomas (Liu et al. 1994; Woronicz et al. 1994). In the thymus, NGFI-B acts upon the T-lymphocytes in both pro-apoptotic (Youn et al. 1999) and anti-apoptotic manners (Suzuki et al. 2003). However, it was recently shown that NGFI-B translocates to mitochondria to initiate the apoptotic process, a function distinct from that carried out by transcription factors (Li et al. 2000). It was shown that the glucocorticoid receptor (GR) and NGFI-B exert mutual antagonism in cells (Philips et al. 1997b). NGFI-B–dependent transcription activity is blunted by increasing concentrations of GR, whereas NGFI-B titrated GR transcription activity on cognate DNA targets in transfection assays (Philips et al. 1997b). NGFI-B was also shown to heterodimerize with other members of NR subfamily 4A (Maira et al. 1999) and with RXR (Forman et al. 1995).

The recent crystallographic structures of Nurr1 and NGFI-B LBDs revealed that these receptors do not have a void in a typical ligand-binding cavity as a result of the tight packing of side chains of several bulky hydrophobic residues in the region normally occupied by ligands. Moreover, the canonical coactivator cleft has hydrophilic rather than hydrophobic topology, indicating that both nuclear receptors lack a classical binding site for coactivators (Wang et al. 2003; Flaig et al. 2005). Furthermore, a novel coregulator interaction surface, composed of helices H11 and H12, has been identified in NGFI-B (Flaig et al. 2005). While the crystal structures of NGFI-B LBD provided a wealth of atomic details of this orphan NR structural organization, we found it necessary to obtain better knowledge of its quaternary structure in solution in order to further understand the role of multimeric assembly in NGFI-B function.

In the present study we report the structural organization of the NGFI-B LBD as revealed by biochemical methods, small-angle X-ray scattering (SAXS) analyses, and hydrogen–deuterium exchange (H/D Ex) experiments followed by mass spectrometry (MS). We retrieved and analyzed ab initio dummy-residue models from SAXS data and used the available crystallographic structures of the isolated NGFI-B LBDs to place them inside the low-resolution envelope, unveiling the most likely dimeric organization of the NGFI-B in solution. The NGFI-B dimerization interface, composed by the loop H2–H3 and the C-terminal part of H3, was unambiguously determined by H/D Ex experiments and revealed unexpected

similarity with the nonclassical dimer interface observed for the glucocorticoid receptor (GR). The similarity of the dimerization mode between these two receptors might be relevant to the ability of GR to inhibit NGFI-B DNA-binding ability and NGFI-B–dependent transcription on a cellular level.

Results and Discussion

Secondary structure of NGFI-B LBD

First, we assessed the folding of recombinant NGFI-B LBD in solution by CD and fluorescence measurements. The measured far-UV CD spectrum at room temperature shows two negative bands at 224 and 209 nm and a positive band near 190 nm (Fig. 1A). Analysis of the spectrum was performed using Dichroweb (Whitmore and Wallace 2004) with the programs SELCON3 (Sreerema et al. 1999), CONTIN (Provencher and Woody 1981), and K2D (Andrade et al. 1993). The α-helical content computed by these programs ranged from 52% to 60%, and that of β-strands, from 4% to 11%. These data are in excellent agreement with the secondary-structure composition calculated on the basis of the crystal structure of NGFI-B LBD, in which the total α-helical content is also ~61%, and total β-strand content, ~4%.

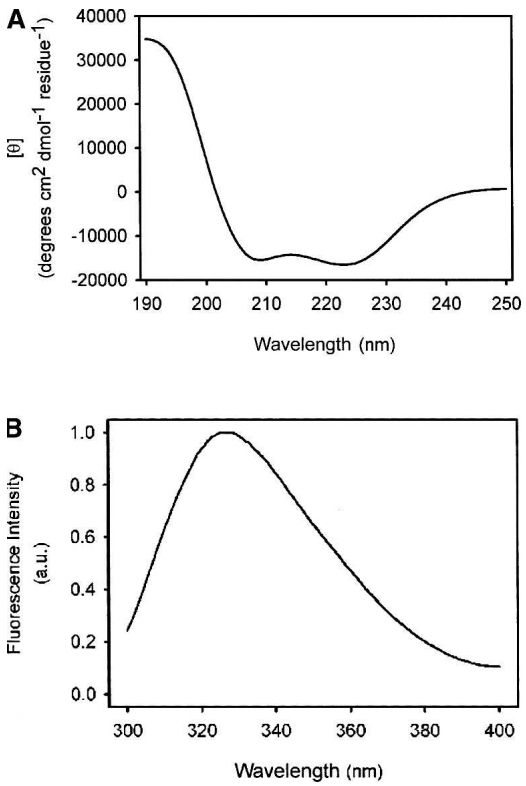

Figure 1. (*A*) Circular dichroism analysis of recombinant NGFI-B LBD. The CD spectra of native NGFI-B LBD at concentration of 0.13 mg/mL in 5 mM phosphate buffer, pH 8.0, plus 1 mM DTT. The spectra were recorded in the range from 190 to 250 nm at room temperature in a 1-mm path-length quartz cuvette using Jasco J-720 spectropolarimeter with an average of 16 scans. (*B*) NGFI-B LBD intrinsic fluorescence spectrum. The emission spectra of NGFI-B LBD were recorded at the excitation wavelength of 280 nm and protein concentration of 0.3 mg/mL in 10 mM phosphate buffer (pH 8.0), 500 mM NaCl, and 1 mM DTT. Experiments were carried out at 25°C and corrected for buffer contribution.

The NGFI-B LBD intrinsic fluorescence emission spectrum has a maximum fluorescence wavelength at 327 nm upon excitation at 280 nm (Fig. 1B), demonstrating that its tryptophan residues are buried. Intrinsic fluorescence emission spectra, recorded during a period of several hours, were practically identical, indicative of stability of the protein at room temperature. Analysis of NGFI-B LBD X-ray structure shows that these residues are hidden within the protein core and are inaccessible to solvent. The accessible surface areas of both conserved tryptophan residues, calculated with the program AREAIMOL from CCP4 program suite (Collaborative Computational Project, Number 4 1994), are 1.0 and 8.4 $Å^2$, which are much smaller as compared to the accessible surface area of the fully solvent-exposed tryptophan residues (111.3 and 113.8 $Å^2$). These results corroborate with the notion of the structural integrity of recombinant NGFI-B LBD in solution.

SAXS data reveal the capacity of NGFI-B to form dimers in solution

To obtain information about NGFI-B LBD quaternary structure and its molecular shape, we submitted this protein to SAXS analysis. Comparative analysis of SAXS scattering curves showed that concentration effects were negligible. Therefore, the SAXS scattering curve, obtained with 6 mg/mL of protein and corrected for the smearing effects, was utilized for structural studies (Fig. 2). Guinier analysis was applied to determine the radius of gyration, R_g = 2.85 nm, for NGFI-B in solution (Fig. 2, lower inset). The same parameter was also obtained from the theoretical fit of the scattering curve by the indirect Fourier transform program GNOM (Fig. 2, upper inset). The radius of gyration and the maximum dimension of the NGFI-B LBD are equal to 2.89 ± 0.10 nm and 9.00 ± 0.50 nm, respectively.

The shape of the protein at 3.14-nm resolution was determined from the X-ray scattering data by two independent procedures (see Materials and Methods). Both ab initio reconstructions rendered very similar V-shaped molecular envelopes. Perfect superposition of the molecular envelope computed on the basis of the spherical harmonics (Svergun et al. 1996, 1997) with the dummy-atom model (DAM) can be observed (Fig. 3). The low-resolution DR model obtained in this study clearly reveals

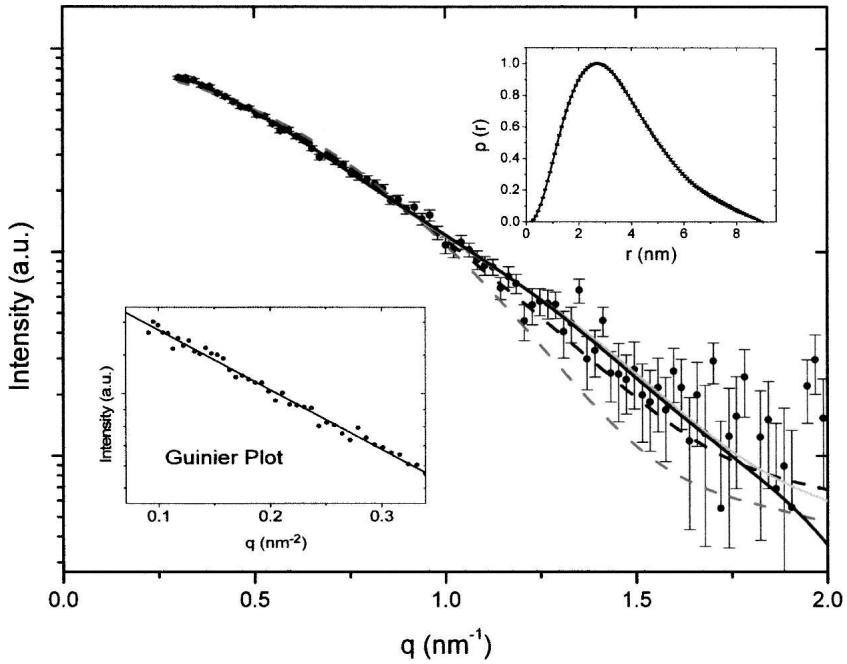

Figure 2. Small-angle X-ray scattering curves for NGFI-LBD. Experimental scattering curves corrected for the smearing effect of NGFI-LBD at 6 mg/mL (black circles with errors bars), with simulated curves corresponding to the low-resolution model (black solid line) and high-resolution model obtained by rigid body adjustment of the symmetrically related NGFI-B LBD dimer (gray solid line), ER LBD (PDB id., 1A52; gray dashed line), and RXRα (PDB id., 1LBD; black dashed line). *Inset below* the scattering curves: Guinier plot with linear fit profiles, allowing the estimation of $R_g = 2.85$ nm. *Upper inset:* NGFI-LBD distance distribution function.

a bilobal molecular envelope characteristic for a dimeric protein (Fig. 3). All of the SAXS-derived structural parameters are consistent with the dimeric organization of the protein in solution at the concentrations used in SAXS experiments. Given the capacity of NGFI-B to recognize monomeric half-sites (NBRE) and, also, to mediate transcription from widely spaced everted palindrome DNA response elements ER10 (NurRE), the ability of this receptor to form dimers in solution is relevant to its physiological function, and we decided to additionally study NGFI-B dimer formation by MS.

MS confirms the existence of NGFI-B dimers

The NGFI-B LBD was submitted to MS analysis, which clearly showed the presence of two protein populations (Fig. 4). The mass envelopes obtained in MS experiments were superposed and corresponded to monomers and dimers of NGFI-B. Deconvolution of the peaks in mass spectra reveals that ~70% of NGFI-B exists as dimers under conditions of the MS experiment with the molecular mass of 62,103 Da, whereas the rest of the protein forms monomers with the molecular mass of 31,126 Da (Fig. 4). The experimentally obtained masses of NGFI-B dimers and monomers closely match the theoretically calculated values of 62,204 and 31,102 Da, respectively. The theoretical calculation of the NGFI-B LBD mass took into account that the construct studied in the present work contained an open reading frame of NGFI-B LBD plus additional amino acid residues derived from the expression vector at its amino terminus, including the cluster of six histidine residues. These results confirm that the protein preferentially forms dimers, which are stable even under the harsh conditions of the MS experiment (see Materials and Methods).

NGFI-B dimer is more open than classical NR homodimers

To evaluate the molecular shape of NGFI-B dimer, we compared its architecture with the properties of the most probable homodimer configurations for two classical nuclear receptor LBDs, ER and RXR. Comparison of the low-resolution shape of NGFI-B with the RXRα and ERα dimer structures shows that, although all three receptors are anisometric, V-like shaped dimers, the angle between the monomers in the low-resolution ab initio model for NGFI-B LBD is significantly larger. The observed angles between RXRα and ERα monomers are 60° and 50°, respectively, whereas the opening angle calculated here for NGFI-B is 140° (Fig. 5A). This also means that the dimer interface for NGFI-B is considerably smaller than the classical dimeric interface found in the crystal structures of RXRα and ERα.

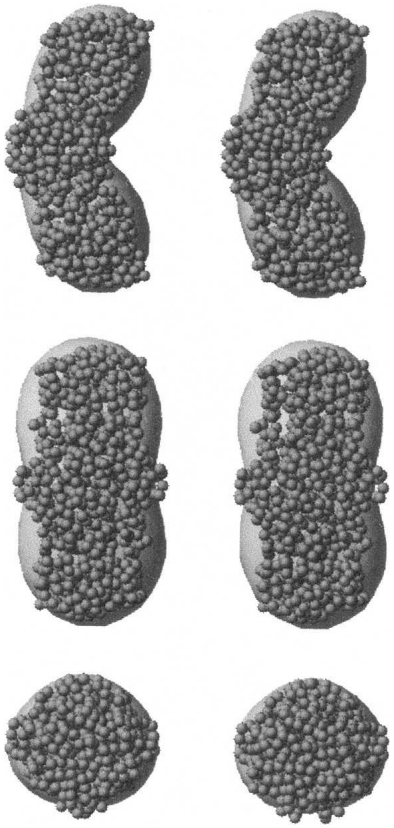

Figure 3. Stereoview of two independently retrieved NGFI B-LBD ab initio low-resolution models. Superposition of the low-resolution envelope, computed by SASHA (Svergun et al. 1996, 1997), with the dummy-atom models, retrieved by GASBOR (Svergun et al. 2001), is given in three projections. *Middle* and *bottom* images are rotated by 90° around the *y* and *x* axes, respectively, compared to the *top* image.

To interpret the SAXS-derived NGFI-B molecular envelope in terms of the high-resolution crystal structures, we compared the envelope with all possible symmetry-related NGFI-B LBD dimers observed in the crystal structure of the protein (Flaig et al. 2005). All six symmetry-related dimers derived from the crystal structure were fitted to the low-resolution molecular envelope (Table 1), presenting χ values of 2.14, 1.52, 1.51, 1.30, 1.25, and 1.22. Although the last three putative dimers showed better χ values and fitted better the low-resolution molecular envelope of NGFI-B, to experimentally map the NGFI-B dimerization surface, we conducted hydrogen–deuterium exchange experiments followed by peptic digestion and MS.

The NGFI–B LBD dimer interface

Part of the surface of the protein involved in the dimeric interface is protected from the solvent upon dimerization. Hence, deuterium uptake at the interface area is hampered in the dimeric assembly, thus opening a possibility for the experimental identification of this interface by MS analysis of the NGFI-B peptides produced by enzymatic digestion. The MS analysis of the NGFI-B LBD peptic digestion identified 40 peptides that cover 91.5% of the protein sequence (data not shown). The H/D exchange occurred in 77% of the protein, with the deuterium incorporation rates in peptides varying between 3% and 100%. The peptides on the surface of the protein that display deuterium protection comprise the H2–H3 loop (14 amino acids), the C-terminal fragment of H3 (eight amino acids), and four amino acids in H10 (Fig. 5B). Mapping of the H/D Ex-protected areas onto the 3D structure of NGFI-B LBD revealed continuous and extended surface area composed by the H2–H3 loop and the C-terminal part of H3. Furthermore, the H2–H3 loop contains a number of hydrophobic residues (L381, Y383, and F386), which are characteristic of the molecular interface. The short four-amino acid fragment of H10 is located at the opposite side of the molecule and neither contains hydrophobic amino acid residues nor forms the continuous surface area. Therefore, the H2–H3 loop and the C-terminal part of H3 clearly mediate NGFI-B dimerization and make part of its dimer interface. Given that, we carefully analyzed the NGFI-B dimers, which were derived from the X-ray structure, looking for the symmetry-related molecules that make contact and interact through the H2–H3 loop and N-terminal part of the H3 interface.

NGFI-B dimer interface is similar, but not identical to, the GR dimer

Only one of the six putative NGFI-B LBD dimers observed in the crystal indeed is formed through the contacts mediated by the H2–H3 loop. Besides, the same dimer has one of the lowest χ values (1.30) in our preliminary SAXS analysis. Since dimer conformation in the crystal lattice could be affected by the crystal contacts, we submitted this dimeric arrangement to rigid-body adjustment against the SAXS data using the SASREF program (Petoukhov and Svergun 2005), yielding an excellent adjustment parameter χ value of 1.14 (Table 1). A putative NGFI-B LDB dimer, which represents the best fit to SAXS data, is given in Figure 5C. Its interface region is characterized mostly by hydrophobic interactions, formed by phenolic rings of the residues Phe386 and Tyr383, and the hydrophobic moiety of the Leu381 side chain. The loss of solvent accessible surface area in the formation of the NGFI-B LBD homodimer is considerably smaller than that for other known nuclear receptor homodimers. RXRα and ERα, for example, lose upon dimerization 1232 and 1672 $Å^2$ of accessible surface, respectively. The accessible surface area hidden by the formation of NGFI-B dimer identified here by SAXS is

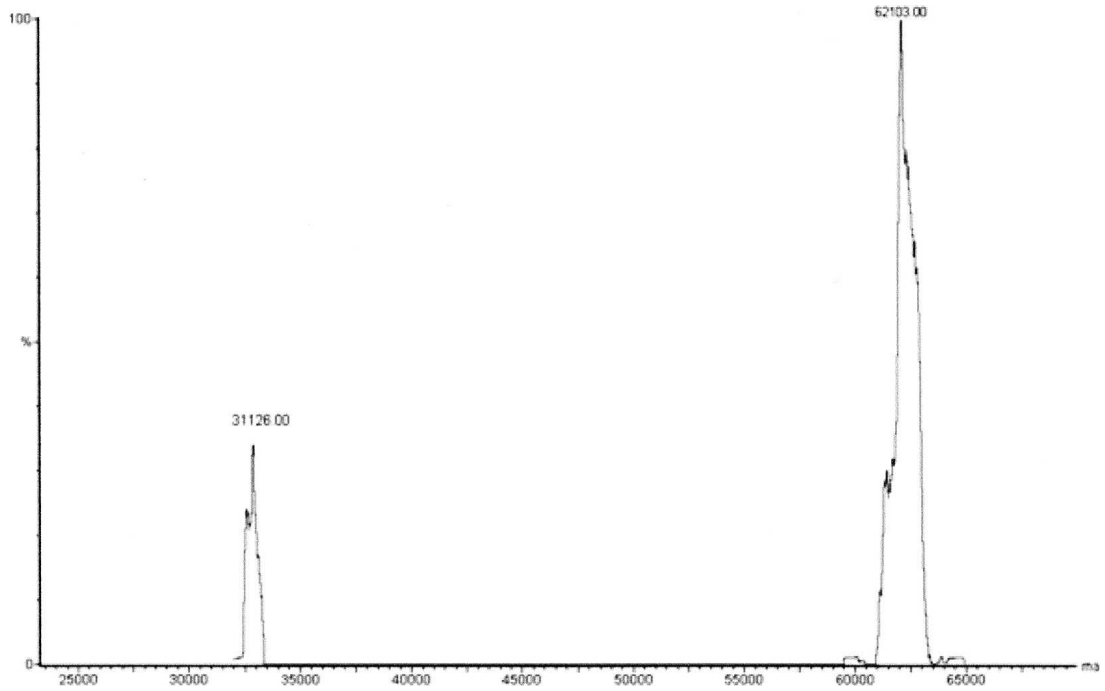

Figure 4. Mass spectrum of NGFI-B after deconvolution. The smaller peak, with molecular mass (MW) of 31,126 Da, corresponds to NGFI-B LBD monomers, and the higher peak corresponds to the dimers with MW of 62,103 Da.

only 579 $Å^2$. (All areas were calculated using the CCP4 program AREAIMOL [Collaborative Computational Project, Number 4 1994].) Another clear difference between the three structures is the dimerization interface. RXRα and ERα LBDs both dimerize through the classical dimerization interfaces, which involves molecular contacts between helices H9 and H10. On the contrary, the NGFI-B LBD dimer interface involves molecular contacts mediated by the H2–H3 loop and C-terminal fragment of the H3 (Fig. 6A,D).

Is the NGFI-B dimerization mode unique? To answer this question we looked carefully at the dimerization interfaces identified for other nuclear receptors. A recent structural study of the glucocorticoid receptor (GR) revealed a new mode of receptor dimerization (Bledsoe et al. 2002; PDB id., 1M2Z), which is mediated by the H2–H3 loop and several residues from β-strands 3 and 4 (Fig. 6B). Although not identical to our NGFI-B dimer model, GR dimerization involves almost the same area on the surface of the receptor (Fig. 6C). The structure-based sequence alignment of NGFI-B, RXR, and GR reveals that the RXR classical dimer interface area comprised by H10 and H11 (Fig. 6D) is much more hydrophobic than the corresponding part of NGFI-B (data not shown). On the other hand, as one would expect, the novel interface region, which includes the H2–H3 loop, is significantly more hydrophobic in GR and NGFI-B structures as compared to RXR.

To analyze the novel NGFI-B LBD dimer in the light of available physiological information, we attempted to investigate a putative mode of the receptor recognition of its DNA response elements NBRE and NurRE.

The NGFI-B quaternary arrangement described here leads to a reduction in the number of intermolecular contacts at the dimerization interface, thus weakening the NGFI-B dimeric assembly. The smaller dimerization interface and weaker dimerization assembly of NGFI-B might be of functional importance for monomeric binding to cognate DNA elements NBRE, which would include molecular contacts between a single NGFI-B DBD and NBRE either in monomeric or dimeric receptor forms.

To propose a model for NGFI-B/NurRE interactions, we decided to study distance constraints imposed by the proposed NGFI-B dimer and the everted palindromic element spaced by 10 base pairs (ER10). Using the crystal structure of NGFI-B DBD complexed with a single half-site DNA element (Meinke and Sigler 1999; PDB id., 1CIT), we constructed a model of two symmetric NGFI-B DBDs bound to ER10 (Fig. 7A). The distance between the two C-terminal helices of NGFI-B DBD motifs AT(G/A)(C/T)CA, spaced by 10 base pairs, in a B-DNA double helix, is 6.7 nm. This value closely matches the distance between the two N-terminal helices H1 in our proposed model of the NGFI-B LBD dimer, which is ~6.9 nm (Fig. 7A). Given the fact that the C-termini of DBDs will be fused with the N-termini of LBDs in a

full-length receptor and allowing for slight positional adjustments, the DBDs of NGFI-B will be perfectly positioned to interact with ER10 in the context of the NGFI-B LBD dimer. To compare these results with other NR LBD and DBD/DNA structures, we analyzed the crystal structures of RXR/RXR LBDs (Bourguet et al. 1995; PDB id., 1LBD) and ER:ER LBDs (Tanenbaum et al. 1998; PDB id., 1A52) homodimers and their corresponding DBD pairs in complex with DNA response elements (Schwabe et al. 1993; Zhao et al. 2000; PDB ids., 1HCQ and 1BY4, respectively). The distance between the two N-termini (H1) of RXR LBD in dimer arrangement is 3.6 nm (Fig. 7B). At the same time, the separation of the C-terminal helices of RXR DBDs complexed to DR-1 DNA response element is 3.7 nm. Similarly, the distance between two N-terminal helices H1 in the ER LBD symmetric dimer is 3.6 nm, compared to the width of 3.4 nm between C-termini of ER DBDs bound to the cognate inverted repeat IR-3 DNA response element (three base pair spaced palindrome; Fig. 7C). As expected, the distances between N-terminal parts of the LBDs dimer match the distances between the corresponding C-termini fragments of the DBDs positioned at the cognate DNA response elements. This further strengthens the notion that the proposed NGFI-B dimer model is well suited for recognition of the widely spaced response elements as the everted palindrome spaced by 10 base pairs (NurRE; Philips et al. 1997a). Moreover, since the novel dimerization interface, involving the H2–H3 loop and part of H3, is on the opposite side of the LBD from the classical dimerization interface (H10) observed in RXR and ER, dimer formation of NGFI-B and GR will involve exposure of a different surface area, such as of a classical dimeric interface, for example. As a consequence, the docking sites for coregulator proteins (corepressors and coactivators), have to be different from those common for receptors dimerizing through the classical interface (ER:ER, RXR:RXR, PPAR:PPAR, RAR:RXR, and PPAR:RXR). This is consistent with the notion of a novel coregulator surface found in NGFI-B and constituted by the residues of H11 and H12 (Flaig et al. 2005). Furthermore, the same surface docking sites available for coregulator interactions might explain a mutual influence of NGFI-B and GR in transcription assays (Philips et al. 1997b). Indeed, GR repression of NGFI-B–dependent transcription could stem from their competition for common protein target (such as coregulators).

It is tempting to speculate that the novel interface revealed by the X-ray structure of GR and combined SAXS H/D Ex analysis of NGFI-B presented here is not restricted to these two receptors and represent a new mode of NR dimerization, particularly as applied to the NR subfamily 4A.

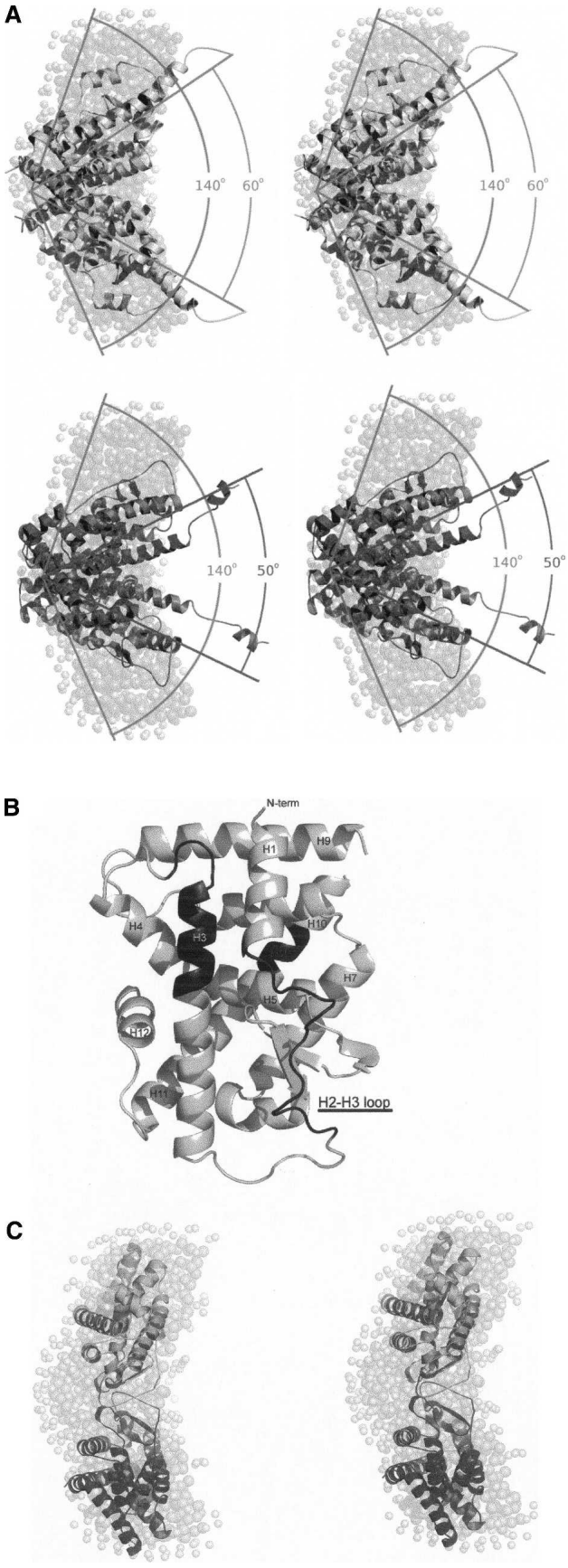

Figure 5. (Legend on next page)

Materials and Methods

Cloning, expression, and purification

The 735-bp sequence of the NGFI-B LBD gene domain (DNA sequence corresponding to amino acids 319–564 in full-length NGFI-B) was inserted into the pET28a(+) expression vector (Novagen). The construct was checked by restriction enzyme assay and transformed into chemically competent *Escherichia coli* strain BL21 (DE3) cells. A single colony obtained on Luria-Bertani (LB)–kanamicin plates was then selected and grown for sequencing using an ABI PRISM 377 DNA Sequencer (AB Applied Biosystems). The BL21 (DE3) cells containing the recombinant vector were grown at 37°C in fresh LB medium at a speed of 250 rpm until absorbance at 600 nm reached 1.0–1.2. Induction was performed at 22°C for 6 h with 1.0 mM isopropyl-β-D-thiogalactopyranoside (IPTG). Cells were then collected by centrifugation, lysed by sonication, and purified by two subsequent steps—affinity and size-exclusion chromatography—using an ÄKTA HPLC system (Amersham Bioscience-GE), resulting in satisfactory protein yields.

Circular dichroism and fluorescence spectroscopy

Circular dichroism spectra were acquired on a Jasco J-720 spectropolarimeter. The protein at a concentration of 0.13 mg/mL was placed in a 1-mm path-length cuvette at room temperature. Spectra were obtained in 5 mM phosphate buffer, pH 8.0, 1 mM DTT; the baseline spectrum (buffer alone) was subtracted from the NGFI-B LBD spectra, and the results were expressed as mean residue ellipticity $[\theta] = (\theta \times \mathrm{MRW})(10 \times c \times d)$, where θ is the observed ellipticity; MRW is the protein mean weight/number of residues; d is the optical path length, in cm; and c is the protein concentration, in mg/mL. The protein far-UV spectra were recorded over a wavelength range from 190 to 250 nm by signal averaging of 16 spectra.

The intrinsic fluorescence of NGFI-B LBD was measured in a 10 mm × 2 mm quartz cuvette at 25°C, using a K2 Multifrequency Phase Fluorometer (ISS). Emission spectra in the range of 300 to 400 nm were recorded using an excitation wavelength of 280 nm. The fluorescence emission spectra of NGFI-B LBD at a concentration of 0.3 mg/mL were monitored at a scanning rate of 1 nm and integration time of 1 s. After each measurement the spectrum was corrected for buffer (10 mM phosphate buffer, pH 8.0, 500 mM NaCl, 1 mM DTT) contribution.

Figure 5. (*A*) Stereoview displaying the superposition of the low-resolution model with dimer structures RXRα LBD (PDB id., 1LBD) (*upper* panel) and ERα LBD (PDB id., 1A52) (*lower* panel). The differences in the dimers opening angles are apparent. (*B*) NGFI-B structure (Flaig et al. 2005; PDB id., 1YJEA) showing the regions protected during H/D Ex experiments (in black): the H2–H3 loop, a fragment of H3, and a fragment of H10. (*C*) Stereoview of superposition of the SAXS-derived DAM low-resolution model of NGFI-B LBD dimer superimposed with the high-resolution dimer observed in the NGFI-B LBD crystal, which obeys the dimeric interface determined in H/D Ex experiments. The chosen NGFI-B LBD dimer was adjusted as a rigid body to the X-ray scattering curves by SASREF (Petoukhov and Svergun 2005).

Table 1. *Structural parameters from SAXS data*

Parameter/sample	Exp[a]	DAM[b]	Mod[c]	RXRα	ERα
R_g (nm)	2.89 ± 0.10	2.75	2.74	2.66	2.41
D_{max} (nm)	9.00 ± 0.50	9.16	9.70	9.44	7.72
Discrepancy, χ	—	1.14	1.14	1.37	1.98
Resolution (nm)[d]	3.14	3.14	—	—	—

[a] Exp, calculated from experimental data.
[b] Dummy-atom model (DAM) parameters with imposed twofold symmetry.
[c] Mod, parameters evaluated from the rigid-body modeling symmetrically related NGFI-B LBD dimer.
[d] Resolution = $2\pi/q_{max}$.

MS experiments

MS experiments were conducted using NGFI-B at 2.4 mg/mL concentration in 50 mM ammonium acetate buffer with 20 mM NaCl at pH 6.8. Mass spectra were collected with the intact protein and with the protein after the pepsin cleavage. This analysis was undertaken to verify the molecular weight of the NGFI-B and to obtain the cleavage pattern of NGFI-B.

H/D Ex was started by the dilution of the protein in the ammonium acetate buffer with 66% of D_2O (pD 7.0) at 4°C, for 1 min. At the specific time, 80 μL of 10 mM phosphate buffer was added to 100 μL deuterated proteins to quench the reaction by lowering the pH to 2.5. Protein cleavage was performed by pepsin addition (0.1 mg/mL diluted in phosphate buffer, pH 2.5) for 10 min, at room temperature. The cleavage reaction was halted by placing the protein on ice.

After addition of 30% acetonitrile, the samples—either the entire protein or the peptides generated by peptic cleavage—were immediately applied onto a Quattro II triple-quadrupole mass spectrometer (Micromass), equipped with a standard ESI source, to avoid back-exchange with solvent hydrogen. The protein mass and the fingerprint of NGFI-B were identified. Analysis of the displacement in peptide peaks identified the fragments of the protein that had undergone H/D exchange. The software program MS-Digest (http://prospector.ucsf.edu/prospector/4.0.8/html/msdigest.htm) (Chalkley et al. 2005) was used to identify the sequence of the peptic peptide ions, generated by pepsin cleavage. The deuterium incorporation level for each peptide was determined from differences in mass centroids between the deutered and nondeutered fragments.

SAXS measurements and data analysis

SAXS data were collected at the small-angle scattering beamline on the LNLS (National Synchrotron Light Laboratory) using multiwire proportional chamber with delay-line readout (Gabriel and Dauvergne 1982). NGFI-B LBD at concentrations 1.5, 3, and 6 mg/mL was measured at a wavelength (λ) of 0.148 nm for sample–detector distances of 732.1 mm covering the momentum transfer range $0.1 < q < 3.4\ \mathrm{nm}^{-1}$ ($q = 4\pi \sin \Theta/\lambda$, where 2Θ is the scattering angle). The scattering curves of the protein solutions and the corresponding solvents were collected in a number of short 100s frames to monitor radiation damage and beam stability. The data were normalized to the intensity of the incident beam and corrected for detector response. The scattering of the buffer was subtracted, and the curves were scaled by concentration. The R_g was approximated by using the Guinier equation (Guinier and Fournet 1955) and GNOM

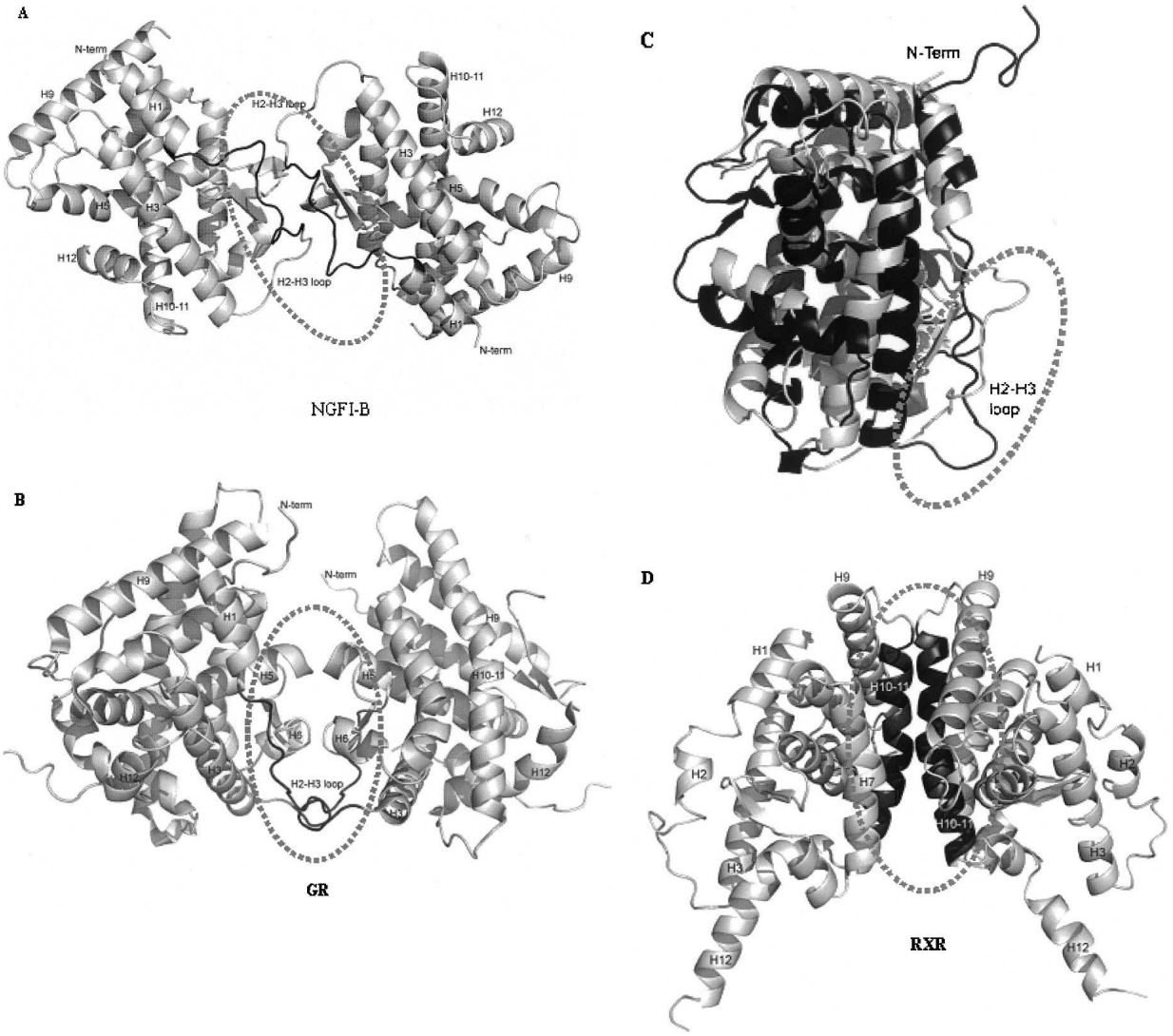

Figure 6. Dimers of NGFI (*A*) and GR (*B*), with the polypeptide fragments that participate in the dimer contacts shown in black. (*C*) Superposition of NGFI-B (in gray) and GR (in black) displaying a similar dimerization interface, involving the H2–H3 loop. (*D*) Classical dimerization interface, exemplified by the RXR dimer, is distinct from the novel dimerization area identified for NGFI-B and GR.

(Svergun 1992). The distance distribution functions $p(r)$ were also evaluated by the indirect Fourier transform program, and D_{max} was obtained.

Low-resolution particle shape was restored from the experimental SAXS data using two independent ab initio procedures. In the first approach, the particle shape was calculated from the SAXS data using a procedure implemented by SASHA (Svergun et al. 1996, 1997). The envelope was represented with spherical harmonics up to $L = 3$ (16 independent parameters), without symmetry restrains. This was justified by the fact that the portions of the scattering curves used for ab initio shape determination using the envelope functions contained $N_s = 6.1$ Shannon channels. The particle shape was also calculated from the SAXS data using procedure implemented by GASBOR (Svergun et al. 2001). DAMs are generated by a random-walk C_α chain and are folded to minimize a discrepancy between the calculated scattering curve from the model and the experimental data.

Several runs of ab initio shape determination with different starting conditions lead to consistent results as judged by the structural similarity of the output models, yielding nearly identical scattering patterns and fitting statistics in a stable and self-consistent process. The final shape restoration was performed using 650 dummy residues assuming P2 molecular symmetry.

Using the allowed space-group symmetry operations for the X-ray structure of NGFI-B LBD (Flaig et al. 2005; PDB id., 1YJE), all the symmetry-related molecules were calculated, resulting in six possible dimer conformations. Simulated scattering curves were obtained for all of these NGFI-B LBD dimer models, for RXRα LBD (Bourguet et al. 1995; PDB id., 1LBD) and for ERα LBD (Tanenbaum et al. 1998; PDB id., 1A52) by CRYSOL (Svergun et al. 1995). Radii of gyration (R_g), maximum intraparticle distances (D_{max}), and discrepancy parameter (χ) were computed by the same program. The conformation of the putative NGFI-B LBD dimer with the intermolecular surface

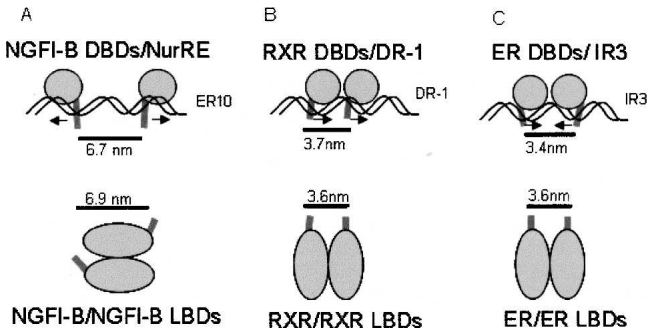

Figure 7. Schematic models (*A*) for the mode of recognition of the everted palindrome spaced by 10 base pairs (ER10, NuRE) by the purposed NGFI-B dimer with nonclassic dimeric interface; (*B*) RXR-RXR DBD bound to DR-1 and the RXR LBD homodimer; and (*C*) ER recognition of the ER response element (IR3). Note a close match of the distances between LBD N-termini H1 and C-termini of the correspondent DBDs on the cognate DNA response elements.

identified in MS experiments was adjusted against SAXS data with the program SASREF (Petoukhov and Svergun 2005). The contact between two symmetrically positioned tryptophane residues (Y383) was maintained during this fitting procedure. SUPCOMB (Kozin and Svergun 2001) was used to superimpose crystallographic structures with ab initio DAMs.

Acknowledgments

We thank Fundação de Amparo de Pesquisa do Estado de São Paulo (FAPESP) for supporting this work (grants 02/05329-6, 02/14041-6, and 06/00182-2) and Conselho Nacional de Desenvolvimento Científico e Tecnológico (CNPq). We thank the Laboratório Nacional de Luz Síncrotron (LNLS) for access to the SAXS beamline and other facilities. I.P., M.S.P., and H.T. are Research Fellows of the Brazilian Counceil for Scientific and Technological Development (CNPq).

References

Andrade, M.A., Chacón, P., Merelo, J.J., and Morán, F. 1993. Evaluation of secondary structure of proteins from UV circular dichroism using an unsupervised learning neural network. *Protein Eng.* **6:** 383–390.

Bledsoe, R.K., Montana, V.G., Stanley, T.B., Delves, C.J., Apolito, C.J., McKee, D.D., Consler, T.C., Parks, D.J., Stewart, E.L., Wilson, T.M., et al. 2002. Crystal structure of the glucocorticoid receptor ligand binding domain reveals a novel mode of receptor dimerization and coactivator recognition. *Cell* **110:** 93–105.

Bourguet, W., Ruff, M., Chambon, P., Gronemeyer, H., and Moras, D. 1995. Crystal structure of the ligand-binding domain of the human nuclear receptor RXR-α. *Nature* **375:** 377–382.

Chalkley, R.J., Baker, P.R., Hansen, K.C., Medzihradszky, K.F., Allen, N.P., Rexach, M., and Burlingame, A.L. 2005. Comprehensive analysis of a multidimensional liquid chromatography mass spectrometry data set acquired on a quadrupole selecting quadrupole collision cell, time-of-flight mass spectrometer. I. How much of the data is theoretically interpretable by search engines? *Mol. Cell. Proteomics* **4:** 1189–1193.

Collaborative Computational Project Number 4. 1994. The CCP4 Suite: Programs for protein crystallography. *Acta Crystallogr.* **D50:** 760–763.

Flaig, R., Greschik, H., Peluso-Iltis, C., and Moras, D. 2005. Structural basis for the cell-specific activities of the NGFI-B and the Nurr1 ligand-binding domain. *J. Biol. Chem.* **280:** 19250–19258.

Forman, B.M., Umesono, K., Chen, J., and Evans, R.M. 1995. Unique response pathways are established by allosteric interactions among nuclear hormone receptors. *Cell* **81:** 541–550.

Gabriel, A. and Dauvergne, F. 1982. The localization method used at EMBL. *Nucl. Instrum. Methods* **201:** 223–224.

Giguere, V. 1999. Orphan nuclear receptors: From gene to function. *Endocr. Rev.* **20:** 689–725.

Guinier, A. and Fournet, G. 1955. *Small-angle scattering of X-rays*. John Wiley and Sons, New York.

Hazel, T.G., Nathans, D., and Lau, L.F. 1988. A gene inducible by serum growth factors encodes a member of the steroid and thyroid hormone receptor superfamily. *Proc. Natl. Acad. Sci.* **85:** 8444–8448.

Herschman, H.R. 1991. Primary response genes induced by growth factors and tumor promoters. *Annu. Rev. Biochem.* **60:** 281–319.

Kozin, M.B. and Svergun, D.I. 2001. Automated matching of high- and low-resolution structural models. *J. Appl. Crystallogr.* **34:** 33–41.

Lee, M.S., Kliewer, S.A., Provencal, J., Wright, P.E., and Evans, R.M. 1993. Structure of the retinoid X receptor α DNA binding domain: A helix required for homodimeric DNA binding. *Science* **260:** 1117–1121.

Li, H., Kolluri, S.K., Gu, J., Dawson, M.I., Cao, X., Hobbs, P.D., Lin, B., Chen, G., Lu, J., Lin, F., et al. 2000. Cytochrome c release and apoptosis induced by mitochondrial targeting of nuclear orphan receptor TR3. *Science* **289:** 1159–1164.

Liu, Z.G., Smith, S.W., McLaughlin, K.A., Schwartz, L.M., and Osborne, B.A. 1994. Apoptotic signals delivered through the T-cell receptor of a T-cell hybrid require the immediate–early gene nur77. *Nature* **367:** 281–284.

Lu, L., Suzuki, T., Yoshikawa, Y., Murakami, O., Miki, Y., Moriya, T., Bassett, M.H., Rainey, W.E., Hayashi, Y., and Sasano, H. 2004. Nur-related factor 1 and nerve growth factor-induced clone B in human adrenal cortex and its disorders. *J. Clin. Endocrinol. Metab.* **89:** 4113–4118.

Maira, M., Martens, C., Philips, A., and Drouin, J. 1999. Heterodimerization between members of the Nur subfamily of orphan nuclear receptors as a novel mechanism for gene activation. *Mol. Cell. Biol.* **19:** 7549–7557.

Maruyama, K., Tsukada, T., Ohkura, N., Bandoh, S., Hosono, T., and Yamaguchi, K. 1998. The NGFI-B subfamily of the nuclear receptor superfamily (review). *Int. J. Oncol.* **12:** 1237–1243.

Meinke, G. and Sigler, P.B. 1999. DNA-binding mechanism of the monomeric orphan nuclear receptor NGFI-B. *Nat. Struct. Biol.* **6:** 471–477.

Milbrandt, J. 1988. Nerve growth factor induces a gene homologous to the glucocorticoid receptor gene. *Neuron* **1:** 183–188.

Perlmann, T. and Jansson, L. 1995. A novel pathway for vitamin A signaling mediated by RXR heterodimerization with NGFI-B and NURR1. *Genes & Dev.* **9:** 769–782.

Petoukhov, M.V. and Svergun, D.I. 2005. Global rigid body modeling of macromolecular complexes against small-angle scattering data. *Biophys. J.* **89:** 1237–1250.

Philips, A., Lesage, S., Gingras, R., Maira, M.-H., Gauthier, Y., Hugo, P., and Drouin, J. 1997a. Novel dimeric Nur77 signaling mechanism in endocrine and lymphoid cells. *Mol. Cell. Biol.* **17:** 5946–5951.

Philips, A., Maira, M., Mullick, A., Chamberland, M., Lesage, S., Hugo, P., and Drouin, J. 1997b. Antagonism between Nur77 and glucocorticoid receptor for control of transcription. *Mol. Cell. Biol.* **17:** 5952–5959.

Provencher, S.W. and Woody, R.W. 1981. Estimation of globular protein secondary structure from circular dichroism. *Biochemistry* **20:** 33–37.

Ribeiro, R.C.J., Kushner, P.J., and Baxter, J.D. 1995. The nuclear hormone receptor gene superfamily. *Annu. Rev. Med.* **46:** 443–453.

Ribeiro, R.C.J., Apriletti, J.W., Wagner, R.L., Feng, W., Kushner, P.J., Nilsson, S., Scanlan, T.S., West, B.L., Fletterick, R.J., and Baxter, J.D. 1998. X-ray crystallographic and functional studies of thyroid hormone receptor. *J. Steroid Biochem. Mol. Biol.* **65:** 133–141.

Saucedo-Cardenas, O., Quintana-Hau, J.D., Le, W.D., Smidt, M.P., Cox, J.J., De Mayo, F., Burbach, J.P., and Conneely, O.M. 1998. Nurr1 is essential for the induction of the dopaminergic phenotype and the survival of ventral mesencephalic late dopaminergic precursor neurons. *Proc. Natl. Acad. Sci.* **95:** 4013–4018.

Schwabe, J.W., Chapman, L., Finch, J.T., and Rhodes, D. 1993. The crystal structure of the estrogen receptor DNA-binding domain bound to DNA: How receptors discriminate between their response elements. *Cell* **75:** 567–578.

Shao, D. and Lazar, M.A. 1999. Modulating nuclear receptor function: May the phos be with you. *J. Clin. Invest.* **103:** 1617–1618.

Sreerema, N., Venyaminov, S.Y., and Woody, R.W. 1999. Estimation of the number of helical and strand segments in proteins using CD spectroscopy. *Protein Sci.* **8:** 370–380.

Suzuki, S., Chuang, L.F., Doi, R.H., and Chuang, R.Y. 2003. Morphine suppresses lymphocyte apoptosis by blocking p53-mediated death signaling. *Biochem. Biophys. Res. Commun.* **5:** 802–808.

Svergun, D.I. 1992. Determination of the regularization parameter in indirect-transform methods using perceptual criteria. *J. Appl. Crystallogr.* **25:** 495–503.

Svergun, D.I., Barberato, C., and Koch, M.H. 1995. CRYSOL—A program to evaluate X-ray solution scattering of biological macromolecules from atomic coordinates. *J. Appl. Crystallogr.* **28:** 768–773.

Svergun, D.I., Volkov, V.V., Kozin, M.B., and Stuhrmann, H.B. 1996. New developments in direct shape determination from small-angle scattering. 2. Uniqueness. *Acta Crystallogr.* **A52:** 419–426.

Svergun, D.I., Volkov, V.V., Kozin, M.B., Stuhrmann, H.B., Barberato, C., and Koch, M.H. 1997. Shape determination from solution scattering of biopolymers. *J. Appl. Crystallogr.* **30:** 798–802.

Svergun, D.I., Petoukhov, M.V., and Koch, M.H.J. 2001. Determination of domain structure of proteins from X-ray solution scattering. *Biophys. J.* **80:** 2946–2953.

Tanenbaum, D.M., Wang, Y., Williams, S.P., and Sigler, P.B. 1998. Crystallographic comparison of the estrogen and progesterone receptor's ligand binding domains. *Proc. Natl. Acad. Sci.* **95:** 5998–6003.

Wang, Z., Benoit, G., Liu, J., Prasad, S., Aarnisalo, P., Liu, X., Xu, H., Walker, N.P.C., and Perlmann, T. 2003. Structure and function of Nurr1 identifies a class of ligand-independent nuclear receptors. *Nature* **423:** 555–560.

Whitmore, L. and Wallace, B.A. 2004. DICHROWEB, an online server for protein secondary structure analyses from circular dichroism spectroscopic data. *Nucleic Acids Res.* doi: 10.1093/nar/gkh371.

Wilson, T.E., Fahrner, T.J., Johnston, M., and Milbrandt, J. 1991. Identification of the DNA binding site for NGFI-B by genetic selection in yeast. *Science* **252:** 1296–1300.

Woronicz, J.D., Calnan, B., Ngo, V., and Winoto, A. 1994. Requirement for the orphan steroid receptor Nur77 in apoptosis of T-cell hybridomas. *Nature* **367:** 277–281.

Wurtz, J.M., Bourguet, W., Renaud, J.P., Vivat, V., Chambon, P., Moras, D., and Gronemeyer, H.A. 1996. A canonical structure for the ligand-binding domain of nuclear receptors. *Nat. Struct. Biol.* **3:** 87–94.

Youn, H.D., Sun, L., Prywes, R., and Liu, J.O. 1999. Apoptosis of T cells mediated by Ca^{2+}-induced release of the transcription factor MEF2. *Science* **22:** 790–793.

Zhao, Q., Chasse, S.A., Devarakonda, S., Sierk, M.L., Ahvazi, B., and Rastinejad, F. 2000. Structural basis of RXR–DNA interactions. *J. Mol. Biol.* **296:** 509–520.